

## Magnetism and Superconductivity in the Rare Earth Nickel Borocarbides

**G. Hilscher and H. Michor,**

*Institute of Solid State Physics, Vienna University of Technology  
Wiedner Hauptstrasse 8-10, A-1040 Vienna, Austria*

**M. EL-HAGARY**

*Physics Department, Helwan University, Helwan, Cairo, Egypt*

**M. DIVIS**

*Department of Electronic Structures, Charles University,  
Ke Karlovu 5, 121 16 Prague 2, Czech Republic*

*The single layer borocarbide and triple layer boronitride superconductors have in common a dual band characteristic at the Fermi level which leads to a complex Fermi surface consisting of several sheets. The theoretical description of the thermodynamic properties and of the upper critical field showing a pronounced upward curvature close to  $T_C$  requires a strong-coupling "Eliashberg" theory which accounts for both the anisotropy of the Fermi surface and the anisotropy of the electron phonon interaction. Using such a theory for conventional electron-phonon mediated polycrystalline superconductors with an *s*-wave order parameter {schachinger} we obtained good agreement with the experimental data with a comparable anisotropy parameter for the Fermi velocity  $\langle b_k^2 \rangle \cong 0.25$  in both systems, the borocarbides and the boronitride, but with a significantly larger anisotropy of electron-phonon interaction  $\langle a_k^2 \rangle \cong 0.08$  for  $La_3Ni_2B_2N_{3-\delta}$  compared to  $\langle a_k^2 \rangle \cong 0.03$  in the single layer borocarbides. The larger  $\langle a_k^2 \rangle$  explains the weak-coupling signatures of the boronitride, though its coupling strength is of similar magnitude as that of the borocarbides, namely, moderately strong.*

Systematic band structure calculations across the series  $RNi_2B_2C$  ( $R = La - Lu$ ) provide valuable results which explain the depression of superconductivity in the light rare earth compounds while magnetic pair-breaking is responsible for the depression of  $T_C$  in the heavy rare earth compounds and their solid solutions with Y and Lu. This is corroborated by an analysis of the specific heat jump at  $T_C$  where the combination of Abrikosov Gor'kov pair-braking in the weak coupling BCS limit with strong coupling corrections explains the quadratic relation between  $\Delta C$  and  $T_C$  reasonably well. Finally, the enhanced pressure dependence of  $T_c$  in the diluted  $Y_{1-x}R_xNi_2B_2C$  compounds with respect to  $YNi_2B_2C$  can be attributed to a pressure induced increase of the exchange interaction  $J_{sf}$ . The corresponding effect of chemical pressure arising from the change of the lattice parameter a due to rare earth substitution is quantitatively in line with that of hydrostatic pressure which provides experimental evidence that  $N(E_f) \cong 0.34$  states / (eV atom spin) and  $J_{sf0} = 31$  meV ( $340$  meV $\text{\AA}^3$ ) is approximately constant within the heavy rare earth compounds.

## 1. Introduction:

The rare-earth transition-metal borocarbides were discovered 1994 [1,2] and attracted attention, because the highest superconducting transition temperatures are comparable to that of the A-15 compounds (as e.g. Nb<sub>3</sub>Ge with  $T_C = 23$  K and on the other hand the interplay of superconductivity and magnetism is reminiscent to the Chevrel-phase superconductors (as e.g. DyMo<sub>6</sub>S<sub>8</sub> or HoMo<sub>6</sub>S<sub>8</sub>). Crystal chemical and substitutional studies quickly reveal a rich variety of possible modifications of the originally reported quaternary rare earth (R) - nickel - borocarbides with  $T_C$  up to 16.5 K for LuNi<sub>2</sub>B<sub>2</sub>C [2]. Siegrist *et al.* [3] reported the crystal structure of the RNi<sub>2</sub>B<sub>2</sub>C superconductors to be a “filled” version of the ThCr<sub>2</sub>Si<sub>2</sub>-type structure stabilized by the incorporation of carbon where Ni<sub>2</sub>B<sub>2</sub> layers are separated by RC layers. Such a layered structure is reminiscent to the high- $T_C$  (HTC) cuprates where superconductivity is supposed to be mediated by properly doped CuO<sub>2</sub>-planes which are separated by rare earth- and/or other metal-oxide layers. However, Mattheiss [4] pointed out that unlike the HTC cuprates, LuNi<sub>2</sub>B<sub>2</sub>C does not have the half-filled sigma-antibonding bands and its electronic structure is almost three-dimensional despite of the layered crystal structure (see also Ref. [5]). As the transition temperature rises with the two-dimensional character in the case of the HTC-materials it was of great interest to investigate modifications of the superconducting properties of intermetallic borocarbides with a more pronounced two-dimensional (layered) crystal structure.

The simplest structural modification of LuNi<sub>2</sub>B<sub>2</sub>C is to incorporate an additional LuC layer yielding (LuC)<sub>2</sub>Ni<sub>2</sub>B<sub>2</sub>. As indicated by the notation chosen, the structure<sup>(1)</sup> of the compound series (LuC)<sub>n</sub>(Ni<sub>2</sub>B<sub>2</sub>) consists of Ni<sub>2</sub>B<sub>2</sub> layers built from NiB<sub>4</sub> tetrahedra separated by n (LuC) rock salt type layers. The two-layer compound (LuC)<sub>2</sub>Ni<sub>2</sub>B<sub>2</sub>, in the following written as LuNiBC, was discovered along with the single-layer RNi<sub>2</sub>B<sub>2</sub>C superconductors [2] and originally reported to be not superconducting. Subsequent investigations on LuNiBC by Gao *et al.* [6] revealed the onset of superconductivity at  $T_C \cong 2.9$  K. Rukang *et al.* [7] prepared further members of the homologous series (YC)<sub>n</sub>(Ni<sub>2</sub>B<sub>2</sub>) with n=3, and 4 but did not find superconductivity down to 4.2 K. Thus, it was speculated that the close contact of Ni<sub>2</sub>B<sub>2</sub> layers in YNi<sub>2</sub>B<sub>2</sub>C is a prerequisite for the appearance of superconductivity.

Lanthanum nickel boronitride compounds (LaN)<sub>n</sub>Ni<sub>2</sub>B<sub>2</sub> with n=2, 3 were reported by Cava *et al.* [8, 9]. These quaternary boronitrides are isostructural with the homologous borocarbide series (YC)<sub>n</sub>Ni<sub>2</sub>B<sub>2</sub> (n=1,...4) [9]. Among the boronitrides superconductivity is observed for La<sub>3</sub>Ni<sub>2</sub>B<sub>2</sub>N<sub>3</sub>

---

<sup>(1)</sup> The structure of (RC)<sub>n</sub>(Ni<sub>2</sub>B<sub>2</sub>) compounds is simple-tetragonal (space group P4/nmm) for n even and body-centered tetragonal (space group I4/mmm) for n odd cite [3].

( $T_C \cong 12$  K) where three LaN rock salt type layers separate the  $\text{Ni}_2\text{B}_2$  layers. The two layer compound  $\text{LaNiBN}$  is reported to be non superconducting down to 4.2 K [8]. Whether the larger separation of the  $\text{Ni}_2\text{B}_2$  layers by three LaN rock salt layers gives rise to a more two dimensional character was discussed theoretically by Mattheiss [10], Singh and Pickett [11]. These band structure results point to rather three-dimensional electronic properties.

The potentially stronger anisotropy of the electronic structure of the triple layer boronitride superconductor  $\text{La}_3\text{Ni}_2\text{B}_2\text{N}_{3-\delta}$  compared to single layer borocarbides can be studied by transport and magnetization measurements on single crystals e.g. via the anisotropy of the upper critical field  $H_{C2}$ . For the borocarbides such studies were reported by various groups, but could not yet be performed for the boronitride due to the severe difficulties to prepare it in single crystalline form. The superconducting properties of  $\text{La}_3\text{Ni}_2\text{B}_2\text{N}_{3-\delta}$  studied by specific heat, magnetization and resistivity measurements on polycrystals [12] reveal a pronounced positive initial curvature of  $H_{C2}(T)$  similar to the borocarbides but its thermodynamic signatures like the exponential temperature dependence of the electronic specific heat  $C_{eS}(T)$  are much closer to the BCS predictions than that of the borocarbides where  $C_{eS}(T)$  is proportional to  $T^3$ . This is remarkable because it proves the s-wave symmetry of the SC order parameter of  $\text{La}_3\text{Ni}_2\text{B}_2\text{N}_{3-\delta}$  while the symmetry of the order parameter of  $\text{YNi}_2\text{B}_2\text{C}$  and  $\text{LuNi}_2\text{B}_2\text{C}$  is still controversial.

## 2. Comparison of the borcarbide and boronitride superconductors

### 2.1 Comparison of electronic properties

The obvious similarity of the crystallographic structures of  $\text{LuNi}_2\text{B}_2\text{C}$  and  $\text{La}_3\text{Ni}_2\text{B}_2\text{N}_{3-\delta}$  they are built by the same  $\text{Ni}_2\text{B}_2$  layers separated by  $\text{LuC}$  or  $(\text{LaN})_3$  rock salt-type layers suggests that at least some features of the electronic structure of the borocarbides and boronitrides should be similar as well. Band structure calculations in fact revealed a dual band characteristics for both, single layer borocarbides and the triple layer boronitride, where essentially two band manifolds contribute to  $N(E_f)$ : broad Ni-B-C (Ni-B-N) s-p bands (30 eV width) and relatively narrow Ni-3d bands (3 eV width) centered slightly below the Fermi level,  $E_f$ , which is situated at a local maximum of electronic density of states (EDOS),  $N(E_f)$ , yielding  $N(E_f)$  4 and 6 states / eV f.u. for  $\text{LuNi}_2\text{B}_2\text{C}$  and  $\text{La}_3\text{Ni}_2\text{B}_2\text{N}_3$ , respectively (see e.g. Refs. [4, 11]).

In a simple rigid band picture metal substitution is expected to shift the Fermi energy relative to the initial value of the parent compound due to the different number of conduction electrons. In the case of  $\text{LuNi}_2\text{B}_2\text{C}$  and  $\text{La}_3\text{Ni}_2\text{B}_2\text{N}_{3-\delta}$  band calculations suggest accordingly that Ni/Co or Cu alloying

will shift the Fermi level out of the local maximum and, thus,  $T_C$  is expected to drop as it was confirmed experimentally. For a quantitative analysis of the influence of Ni/Co or Cu substitution upon the EDOS of the borocarbide and boronitride superconductors we compared specific heat and magnetic susceptibility data of  $Y(Ni_{1-x}Co_x)_2B_2C$  (Ref. [13]) and  $La_3(Ni_{1-x}M_x)_2B_2N_{3-\delta}$  with  $M = Co, Cu$  [14]. As expected from the observed suppression of superconductivity in both systems calorimetry reveals a systematic decrease of the electronic specific heat,  $C_{el} = \gamma T$  which is related to the reduction of  $N(E_f)$  due to Ni/Co substitution. Quantitatively, one finds approximately the same effect  $\delta N(E_f)/\delta x \cong -0.1$  states/(eV f.u. mol Co) in both systems.

Accordingly, both band structure and Ni-site substitution studies indicate that the electronic properties related to the  $Ni_2B_2$  layers are rather similar in both systems, though the complex shape of the Fermi surface of the single layer borocarbides and triple layer boronitride is certainly different.

## 2.2 Comparison of superconducting state properties

The characterization of SC state properties of  $La_3Ni_2B_2N_{3-\delta}$  was performed on polycrystalline samples including thermodynamic properties like the temperature dependence of the electronic specific heat and of thermodynamic and upper critical fields,  $H_C(T)$  and  $H_{C2}(T)$  [12]. Thus, we compare in Fig. (1) the SC state electronic specific heat  $C_{es}(T)$  and  $H_{C2}(T)$  of  $La_3Ni_2B_2N_{3-\delta}$  with data obtained on polycrystalline  $LuNi_2B_2C$  [15].

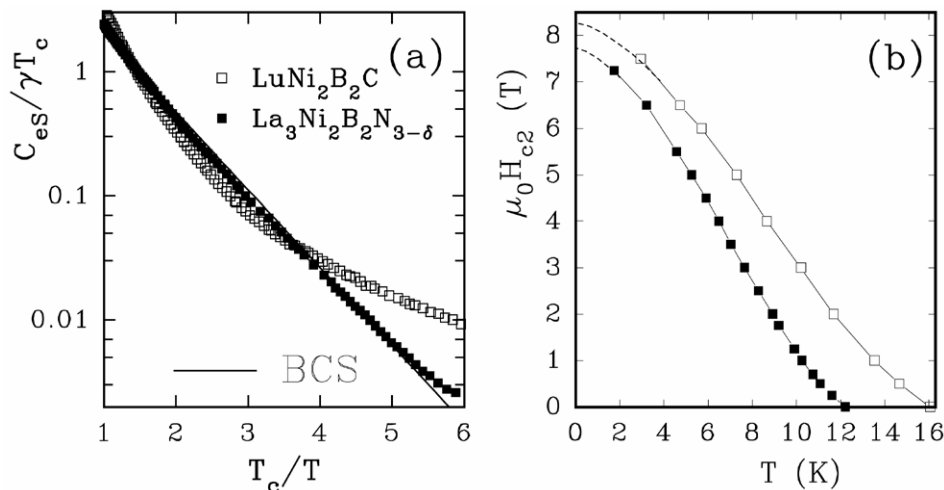


**Fig. (1) :** Comparison of the electronic specific heat  $C_{es}(T)$  in a semi-logarithmic plot in (1a) and the upper critical field  $H_{C2}(T)$  in (1b) for  $La_3Ni_2B_2N_{3-\delta}$  and  $LuNi_2B_2C$ .

As demonstrated by the semi-logarithmic graph of  $C_{es}(T)$  in Fig. (1a),  $\text{La}_3\text{Ni}_2\text{B}_2\text{N}_{3-\delta}$  exhibits an exponential temperature dependence,  $C_{es}(T) = 8.5\gamma T_C \exp(-0.82\Delta(0)/k_B T)$ , with a gap to critical temperature ratio  $\Delta(0)/k_B T_C \cong 1.85$  which is close to the BCS value of 1.76. Accordingly, the symmetry of the SC order parameter of the boronitride is of s-wave type.  $\text{LuNi}_2\text{B}_2\text{C}$  on the other hand shows a cubic temperature dependence,  $C_{es} \propto T^3$  which may arise from a gap function with nodal points on the Fermi surface. Nodal points are not a characteristic of d-wave symmetry where line nodes (yielding a quadratic temperature dependence of  $C_{es}(T)$ ) are expected. A possible explanation of  $C_{es} \propto T^3$  may be the complex Fermi surface (FS) topology consisting of three separate sheets [16] where Terashima et al. [17] reported a significantly reduced gap for the smallest one an electron pocket around the  $\Gamma$ -point. The small (or may be even vanishing) gap on this FS pocket together with an s-wave gap on the two other Fermi surface parts eventually explain the cubic temperature dependence of  $C_{es}$  of Y- and  $\text{LuNi}_2\text{B}_2\text{C}$ .

The upper critical fields,  $H_{C2}(T)$ , of  $\text{LuNi}_2\text{B}_2\text{C}$  and  $\text{La}_3\text{Ni}_2\text{B}_2\text{N}_{3-\delta}$  in Fig. (1b) exhibit a very similar temperature dependence with an unconventional positive curvature close to  $T_C$  – unconventional in the sense that this feature can not be explained by any isotropic single band BCS or Eliashberg model which give a constant slope of  $H_{C2}(T)$  close to  $T_C$ . Thus, Shulga et al. [18] suggested an isotropic two-band approach for  $\text{YNi}_2\text{B}_2\text{C}$  and  $\text{LuNi}_2\text{B}_2\text{C}$  with Fermi velocities  $v_{F1} \sim 0.9 \times 10^5$  m/s and  $v_{F2} \sim 3.8 \times 10^5$  m/s. Since the borocarbides and the boronitride show the same dual band characteristic at the Fermi level, it is obvious that the two-band model shall also explain the temperature dependence of  $H_{C2}$  of  $\text{La}_3\text{Ni}_2\text{B}_2\text{N}_{3-\delta}$ .

In order to analyze the thermodynamic results and upper critical field data by one set of parameters we applied the theory of  $H_{C2}(T)$  for anisotropic polycrystalline superconductors developed by Prohammer and Schachinger [19] using realistic Eliashberg functions  $\alpha^2 F(\omega)$  evaluated via the lattice heat capacities [20]. The model employs a separable ansatz for the anisotropy of the electron-phonon interaction,  $[\alpha^2 F(\omega)]_{k,k'} = (1+a_k)\alpha^2 F(\omega)(1+a_{k'})$  where the mean-square  $\langle a_k^2 \rangle$  is the parameter characterizing the anisotropy of  $\alpha^2 F(\omega)$  and an ansatz  $v_{F,k} = (1+b_k)\langle v_F \rangle$  for the anisotropy of the Fermi velocity, where the mean Fermi velocity  $v_F$  and its mean-square anisotropy parameter  $b_k^2$  account for the shape of the Fermi surface. It has to be noted, that the isotropic two-band and anisotropic single band approach are in some degree technically equivalent, because the separable ansatz employed by Prohammer and Schachinger [19] can be described in its simplest form by a Fermi surface split into two half-spheres of equal weight.

As expected from the success of the isotropic two-band model used by Shulga *et al.* [18],  $H_{C2}(T)$  of  $\text{LuNi}_2\text{B}_2\text{C}$  and  $\text{La}_3\text{Ni}_2\text{B}_2\text{N}_{3-\delta}$  is well described also by the anisotropic single band approach yielding mean Fermi velocities  $v_F \cong 29 \times 10^5$  m/s and  $23 \times 10^5$  m/s, respectively, and practically the same mean-square anisotropy parameter  $b_k^2 \cong 0.25$ . The latter shows that  $b_k^2$  accounts for the different Fermi velocities of the Ni-B-C/N s-p band and Ni-3d bands rather than for a spatial anisotropy expressed by  $v_x:v_z$  which was calculated to be nearly one in the case of  $\text{LuNi}_2\text{B}_2\text{C}$  [11]. From the match of the FS anisotropy parameter  $b_k^2$  which mainly follows from  $H_{C2}(T)$  one may conclude that the structural difference of the single versus triple layer in between the  $\text{Ni}_2\text{B}_2$  planes is of minor importance. However, the simultaneous consideration of the thermodynamic data e.g. of the deviation function of the thermodynamic critical field,  $D(T/T_C)$ , shown in Fig. (2) requires a significantly larger anisotropy of the electron-phonon interaction  $a_k^2 \cong 0.08$  for  $\text{La}_3\text{Ni}_2\text{B}_2\text{N}_{3-\delta}$  compared to  $a_k^2 \cong 0.03$  for Y- or  $\text{LuNi}_2\text{B}_2\text{C}$  [20]. When increasing the anisotropy parameter  $a_k^2$  for given electron phonon coupling factor  $\lambda$  one finds an increase of the upper critical field  $H_{C2}(0)$  on the one hand and a change of the thermodynamic signatures as  $D(T/T_C)$  or the BCS ratios (e.g.  $\Delta C/\gamma T_C$ ) towards the weak-coupling predictions. Thus, the larger anisotropy  $a_k^2$  of the boronitride explains why its thermodynamic signatures are much closer to the BCS predictions than that of the borocarbides though they have similar electron phonon coupling factors ( $\lambda \cong 0.9$ ) for  $\text{La}_3\text{Ni}_2\text{B}_2\text{N}_{3-\delta}$  compared to  $\lambda \cong 1.0$  and  $1.2$  for Y- and  $\text{LuNi}_2\text{B}_2\text{C}$  and also a similar magnitude of  $H_{C2}(0)$  despite of the lower  $T_C$  of the nitride. We note, that a consistent description of the thermodynamic properties and the upper critical field of the borocarbides and the boronitride within the Eliashberg theory is achieved *only*, if anisotropy (or multi-band) effects of the electron-phonon coupling and of the Fermi velocity are included.

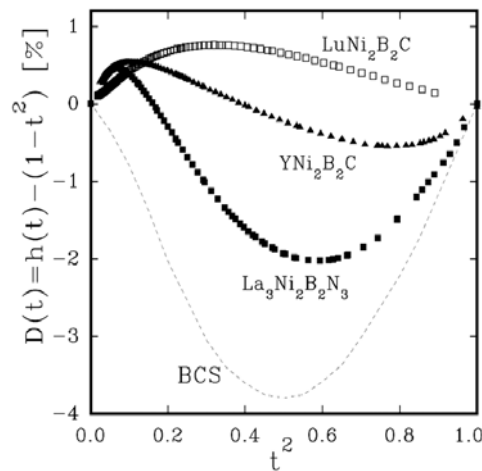


Fig. (2) : Comparison of the deviation functions  $D(t) = [H_c(t)/H_c(0)] [1-t^2]$  with  $t=T/T_c$  of the single layer borocarbides and  $\text{La}_3\text{Ni}_2\text{B}_2\text{N}_{3-\delta}$ .

### 3. Coexistence of Superconductivity and Magnetism

The rare earth nickel borocarbides  $RNi_2B_2C$  compounds and their related pseudoquaternaries are ideal materials for studies of the interplay between long range magnetic order and superconductivity since the Neel temperatures,  $T_N$ , are of the same order of magnitude as the superconducting transition temperatures  $T_C$ . Magnetism coexists with superconductivity in  $RNi_2B_2C$  for  $R = Dy, Ho, Er$  and  $Tm$  [21] whereas only antiferromagnetic order occurs for  $R = Pr, Nd, Sm, Gd$  and  $Tb$  (see e.g. [22, 23]). The approximate scaling of  $T_N$  with the de Gennes factor,  $DG = (g_J - 1)^2 J(J+1)$ , across the series provides evidence that the coupling between the local  $4f$  moments proceeds in terms of the RKKY interaction via conduction electrons rather than by dipolar interactions. The coexistence and the fairly weak coupling of superconductivity and magnetism is attributed to the different extent of electron localization in the borocarbides. Band structure calculations [4, 5, 24] show that the density of states at the Fermi energy  $N(E_f)$  arises mainly from the Ni-3d electrons which are believed to be responsible for superconductivity in these compounds. The interplay between magnetism and superconductivity is mediated by the itinerant electrons.

The depression of superconductivity in  $RNi_2B_2C$  and in the related pseudoquaternary systems  $Y_{1-x}R_xNi_2B_2C$  and  $Lu_{1-x}R_xNi_2B_2C$  (where  $R$  is a heavy rare earth) scales roughly with the DG factor and follows for the latter in the dilute limit the Abrikosov Gor'kov pair-breaking relation  $\ln(T_C/T_C^0) = \Psi[(T_C^0/2T_C)\rho + 1/2] - \Psi(1/2)$  where  $T_C$  and  $T_C^0$  are the critical temperatures with and without magnetic impurities and  $\Psi$  is the digamma function. The pair-breaking parameter  $\rho = [cN(E_f)J_{sf}^2(g_J - 1)^2 J(J+1)] / (k_B T_C^0)$  contains the concentration  $c$  of the magnetic impurities, the  $s$ - $f$  exchange interaction,  $J_{sf}$ , the density of states at the Fermi level and the DG factor. In the dilute limit and the absence of CEF effects the depression of  $T_C$  is expected to follow a de Gennes scaling as long as  $N(E_f)$  and  $J_{sf}$  remain fairly constant across the series. Fulde and Peschl [25] provided an appropriate extension of the AG pair-breaking theory which properly includes CEF effects:  $J(J+1)$  is replaced by  $[J(J+1)]_{eff}$  which incorporates the transitions between the ground and the excited CEF states. A numerical evaluation of  $[J(J+1)]_{eff}$ , however, predicts a minor influence of the CEF upon the DG factor [26]. It is well known from the ternary systems that the DG scaling of  $\Delta T_C$  is reasonably well fulfilled even for higher concentrations if there exists only a weak hybridization between the  $4f$  states and conduction electrons. Significant deviations, however, are observed for the concentrated regime which result in remarkable deviations or even a breakdown of the de Gennes scaling for  $T_C$  in particular for systems  $R_{1-x}R_xNi_2B_2C$  where  $T_N > T_C$  but also in some cases in the paramagnetic regime where  $T_C > T_N$  [23,26,27]. Nevertheless, in view of the approximate de Gennes

scaling of  $T_C$  for the magnetic heavy rare-earth superconductors one expects that superconductivity should occur also in the light rare-earth borocarbides as long as electronic changes are not taken into account for the disruption of superconductivity. In the following we discuss the influence of pair-breaking of the localized  $4f$ -moments upon the depression of superconductivity together with variations of  $N(E_f)$  across the rare earth series  $RNi_2B_2C$ , its influence upon thermodynamic quantities as the specific heat jump and the effect of chemical and hydrostatic pressure upon  $J_{sf}$  and the reduction of  $T_C$  in the pseudoquaternaries  $R_{1-x}R_xNi_2B_2C$  ( $R = Y, Lu$ ).

### 3.1 The relation between the superconducting transition temperature

#### $T_C$ and electronic density of states $N(E_f)$

Mattheiss et al. [10] pointed out that the variation of the B-Ni-B angle has a drastic influence upon  $N(E_f)$  which explains the disappearance of superconductivity in  $LaNi_2B_2C$ . Therefore, a systematic band structure study across the rare-earth borocarbide series has been performed by Divis et al. [24] which shows that  $N(E_f)$  decreases significantly in the light rare earth with respect to the heavy rare earth borocarbides  $RNi_2B_2C$  ( $R = Tb, \dots, Lu$ ).

In a first approach, using the McMillan formula, one can estimate  $T_C$  by rescaling the electron phonon mass enhancement  $\lambda = N(E_f)\langle I^2 \rangle / M\langle \omega^2 \rangle$  across the rare earth series: With  $N(E_f)^{Lu} = 4.06$  states/eV f.u. and  $\lambda^{Lu} = 1.15$  for  $LuNi_2B_2C$  the electron phonon enhancement of the particular compound can be rescaled by  $\lambda^R = \lambda^{Lu} x N(E_f)^R / N(E_f)^{Lu}$  under the assumption that the average electron phonon matrix element  $\langle I^2 \rangle$  remains fairly constant and that the mean atomic mass  $M$  balances the change of the characteristic phonon frequency  $\langle \omega^2 \rangle$  across the series. Thus, the superconducting transition temperatures  $T_{C0}^R$  without magnetic pairbreaking estimated with the McMillan formula  $T_{C0}^R \propto \exp\{-1.04[1+\lambda^R]/(\lambda^R - \mu^* [1+0.62\lambda^R])\}$  are plotted together with the  $N(E_f)$  values obtained from DFT calculations [24] in Fig. (3a). The reduction of  $N(E_f)$  on the light rare earth side is large enough to reduce  $T_C$  to about 3 K for  $LaNi_2B_2C$ , while  $N(E_f)$  and  $T_{C0}^R$  remains rather constant in the heavy rare earth compounds. As shown in Fig. (3a) the density of states at  $E_f$  determined from specific heat measurements is in good agreement with the calculated value for  $LaNi_2B_2C$  and  $LuNi_2B_2C$ . The fact that  $LaNi_2B_2C$  is not superconducting above 20 mK provides according to the McMillan formula an upper limit for  $\lambda^{La} \leq 0.35$  which is significantly smaller than the rescaled value  $\lambda^{La} N(E_f) = 0.65$  obtained with the above procedure. This implies that not only  $N(E_f)$  but also  $\langle I^2 \rangle$  drops concomitantly due to changes of the band structure in the light rare earth compounds. For more details concerning the calculation of the mean electron phonon matrix element  $\langle I^2 \rangle$  in terms of the rigid muffin-tin approximation (RMTA) and the uncertainty of the absolute  $\lambda$  value with respect

to  $\langle \omega^2 \rangle$  we refer to Ref. [24]. Shown in Fig. 3b is the variation of the Hoppfield parameter  $\eta_\alpha = N_\alpha(E_f) \langle I_\alpha^2 \rangle$  where  $N_\alpha(E_f)$  is the site projected density of states for the particular atom ( $\alpha = R, \text{Ni}, \text{B}, \text{C}$ ). This provides a good argument that the simple rescaling of  $T_{c0}^R$  is a reasonable approximation and that the drop of  $\eta$  contributes to a further reduction of  $T_{c0}^R$  in the light rare earth compounds with  $R = \text{La}, \text{Pr}, \text{Nd}$  and  $\text{Sm}$ .

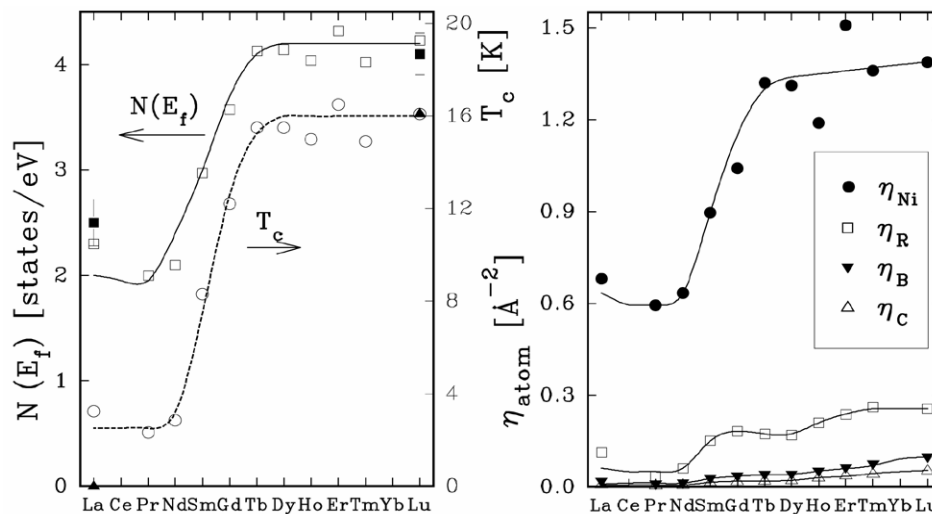


**Fig. (3)** : The calculated  $N(E_f)$  and the superconducting transition temperatures  $T_{c0}^R$  rescaled according to the McMillan formula (see text). Full squares: the experimental  $N(E_f)$  values for  $R = \text{La}$  and  $\text{Lu}$  derived from the electronic specific heat. Full triangles: the experimental  $T_c$  values for  $\text{La}$  and  $\text{LuNi}_2\text{B}_2\text{C}$  (a). The Hoppfield parameters  $\eta_\alpha$  obtained by the RMTA approach; full lines are guide for the eye (b).

We conclude that magnetic pair-breaking is the reason for the suppression of superconductivity in  $\text{GdNi}_2\text{B}_2\text{C}$  and  $\text{TbNi}_2\text{B}_2\text{C}$  due to the large DG factor because  $N(E_f)$  is of the same magnitude as for the corresponding  $\text{Lu}$  and  $\text{Y}$  compounds. On the other hand, the reduction of  $N(E_f)$  and  $\eta$  is detrimental for the occurrence of superconductivity in  $\text{RNi}_2\text{B}_2\text{C}$  with  $R = \text{La}, \text{Pr}, \text{Nd}$  and  $\text{Sm}$ .

### 3.2 The effect of magnetic impurities upon the specific heat anomalies

The interplay of magnetism and superconductivity was investigated by various techniques (see e.g. [23] and references therein). A calorimetric characterization of the superconducting state of the magnetic borocarbides, however, is hindered by the large magnetic background heat capacity. Not even a rough estimation of the normal-state parameters like the electronic specific

heat or the Debye temperature can be performed as can be seen from Fig. (4) where for  $Y_{1-x}Er_xNi_2B_2C$  the magnetic contribution exceeds the specific heat jump at  $T_C$  already for  $x > 0.4$ . On the other hand, the specific heat jump associated with the superconducting transition  $\Delta C_{TC} = C_s(T_C) - C_n(T_C)$  being one of the important quantities to characterize the superconducting state, is reduced by magnetic pair-breaking. For details of the evaluation of  $\Delta C$  we refer to Ref. [28].

In the framework of the BCS theory, thermodynamic quantities adopt universal values as e.g. the normalized specific heat jump  $\Delta C/\gamma T_C = 1.43$ . Accordingly,  $\Delta C$  should vary linearly with  $T_C$  as long as  $\gamma$  remains constant in a series of compounds as it should be in the case for the heavy rare earth borocarbides and their solid solutions with Y and Lu. The variation of  $\Delta C$  versus the normalized transition temperature of  $Y_{1-x}R_xNi_2B_2C$  displayed in Fig. (5) shows that the reduction of  $T_C$  is accompanied by a rather systematic drop of  $\Delta C$  which is stronger than the linear correlation of  $\Delta C$  and  $T_C$  expected from the BCS theory. The specific heat jump versus the normalized temperature of the solid solutions as well as the boundary compounds follows an almost quadratic relation  $\Delta C \propto T_C^\alpha$  with  $\alpha = 1.96(5)$  shown in Fig. 5 by the dashed line. The influence of paramagnetic impurities upon a BCS superconductor has been calculated in terms of the AG pair-breaking theory by Skalski *et al.* [29] yielding a significant deviation of the thermodynamic ratio  $\Delta C/\gamma T_C$  from the linear BCS relation and represents a universal function of  $T_C/T_{C0}$  which incorporates the pair-breaking parameter. This result is the dotted line denoted by (AG) in Fig. (5) and corresponds to an approximate power law  $\Delta C \propto T_C^\alpha$  with  $\alpha = 1.56$ . The experimental data, however, are significantly larger than the AG calculation in the BCS weak coupling limit particularly for  $T_C/T_{C0} > 0.6$  which indicates that strong coupling effects have to be taken into account. Strong coupling effects renormalise the thermodynamic BCS ratios as summarised in form of approximate equations by Carbotte [30] e.g. the normalized specific heat jump is given by

$$\Delta C / \gamma T_C = 1.43 [1 + 53(T_C / \omega_n)^2 \ln(\omega_n / 3T_C)].$$

The strong coupling parameter is the ratio  $T_C / \omega_n$  where the characteristic phonon frequency  $\omega_n$  is the logarithmic moment of a weighted phonon density of states. The ratios  $\Delta C / \gamma T_C$  of the non-magnetic superconductors  $\text{YNi}_2\text{B}_2\text{C}$  and  $\text{LuNi}_2\text{B}_2\text{C}$  were determined to be 1.83 and 2.1 which shows that these compounds are moderately strong coupled electron phonon superconductors with  $\omega_n = 290$  K and 190 K, respectively [23]. The strong coupling relation is displayed as the dashed line (denoted SCR) in Fig. (5) where we use for the Y-based solid solutions  $\gamma = 19.7$  mJ/molK<sup>2</sup> and  $T_{C0} = 15.54$  K of  $\text{YNi}_2\text{B}_2\text{C}$ . The combination of the magnetic pair-breaking in the BCS limit with strong coupling corrections (i.e. AG\*SCR) represented by the full line in Fig. (5) yields an approximate power law  $\Delta C = T_C^\alpha$  with  $\alpha = 1.9$  being close to the nearly quadratic relation ( $\alpha = 1.96$ ) observed experimentally. The overall agreement of this simple approach with our experimental data indicates that the  $\gamma$  value and hence the electronic density of states is almost constant in the heavy rare earth borocarbides and their pseudoquarternary solid solutions with Y which is inline with the above mentioned band structure calculations.

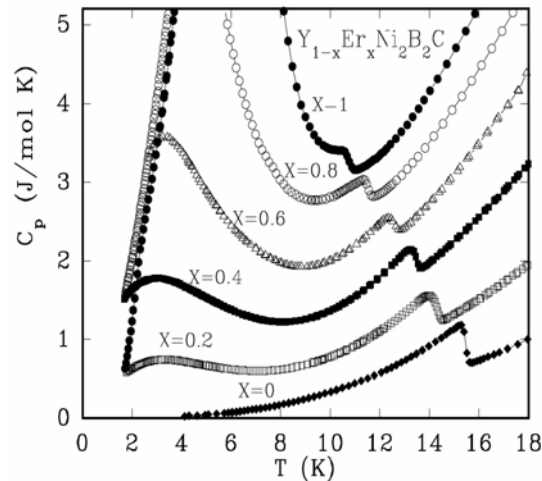


**Fig. (4):** Specific heat of  $\text{Y}_{1-x}\text{Er}_x\text{Ni}_2\text{B}_2\text{C}$  as a function of temperature for various concentrations  $x$ .

where we use for the Y-based solid solutions  $\gamma = 19.7$  mJ/molK<sup>2</sup> and  $T_{C0} = 15.54$  K of  $\text{YNi}_2\text{B}_2\text{C}$ . The combination of the magnetic pair-breaking in the BCS limit with strong coupling corrections (i.e. AG\*SCR) represented by the full line in Fig. (5) yields an approximate power law  $\Delta C = T_C^\alpha$  with  $\alpha = 1.9$  being close to the nearly quadratic relation ( $\alpha = 1.96$ ) observed experimentally. The overall agreement of this simple approach with our experimental data indicates that the  $\gamma$  value and hence the electronic density of states is almost constant in the heavy rare earth borocarbides and their pseudoquarternary solid solutions with Y which is inline with the above mentioned band structure calculations.

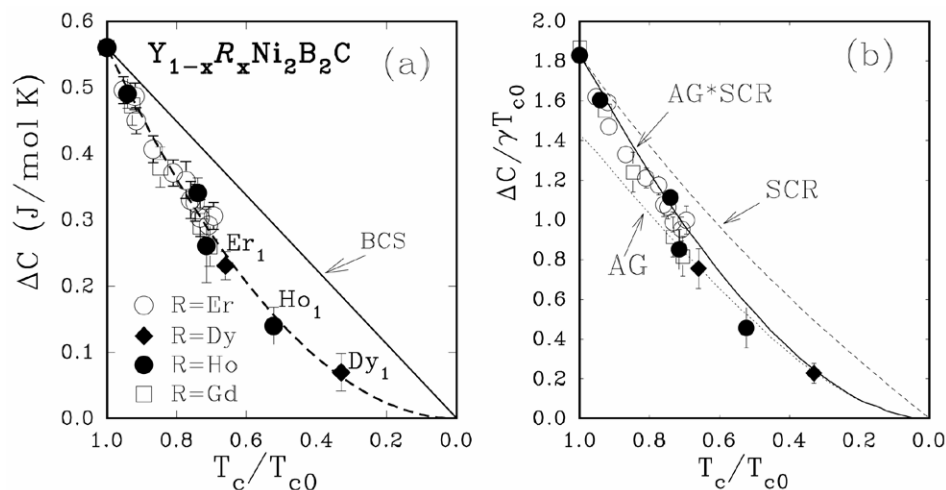


**Fig. (5) :** Variation of the specific heat jump  $\Delta C$  versus the normalized temperature  $T_c/T_{c0}$  for  $Y_{1-x}R_xNi_2B_2C$  where  $R$  is the particular rare earth as labeled. The solid line indicates the linear BCS relation where  $\gamma$  is assumed to be constant; the dashed line corresponds to  $\Delta C \propto T_c^{1.96}$  (a). The ratio  $\Delta C/\gamma T_{c0}$  as a function of  $T_c/T_{c0}$  for  $Y_{1-x}R_xNi_2B_2C$  ( $R= Gd, Dy, Ho$  and  $Er$ ); the dashed line represents the strong coupling relation (SCR), the dotted line the AG result and the solid line the combination of both AG\*SCR (b).

### 3.3 The effect of chemical and hydrostatic pressure upon pair-breaking in magnetic borocarbide superconductors

High pressure studies of the non-magnetic superconductors  $YNi_2B_2C$  and  $LuNi_2B_2C$  revealed a rather small pressure effect upon  $T_c$  ranging from  $dT_c/dp \cong -90$  to  $+3.2$  mK/Kbar [31,32]. This indicates that the pressure induced lattice stiffening is small in these systems or is probably compensated by electronic effects. Thus, magnetic  $RNi_2B_2C$  superconductors are considered to be ideal compounds to study the effect of hydrostatic pressure upon the pair-breaking exchange interaction with the  $4f$ -electrons  $J_{sf}$ .

Resistivity measurements under hydrostatic pressure on  $R_{1-x}R_xNi_2B_2C$  with  $R = Y, Lu$  and  $R = Gd$  and  $Dy$  reveal in the dilute regime ( $x < 0.4$ ) a significant pressure effect upon  $T_c$  although  $T_c$  of  $Y$ - and  $LuNi_2B_2C$  is nearly pressure independent. The analysis of  $T_c(p)$  of several dilute compounds  $Y_{1-x}R_xNi_2B_2C$  with a modified Abrikosov Gor'kov relation taking the pressure dependence into account by  $J_{sf}(p) = J_{sf}(0) + (dJ_{sf}/dp)P$  yields a common set of parameters  $J_{sf}(0) \cong 36$  meV (see footnote <sup>2</sup>).

<sup>2</sup> The frequently used dimension of  $J_{sf}$  [ $eV\text{\AA}^3$ ] is obtained by multiplying the value  $J_{sf} \cong 36$  meV by the mean atomic volume  $V_{atom} = 10.8 \text{\AA}^3$  yielding  $J_{sf} = 390$  meV $\text{\AA}^3$  and  $dJ_{sf}/dp \cong 0.13$  meV/kbar which indicates a rather systematic effect of hydrostatic pressure upon the exchange coupling. Accordingly a similar variation of  $J_{sf}$  is anticipated for the

An estimate of the relative increase of chemical pressure in  $\text{Lu}_{1-x}\text{Gd}_x\text{Ni}_2\text{B}_2\text{C}$  with respect to  $\text{Y}_{1-x}\text{Gd}_x\text{Ni}_2\text{B}_2\text{C}$  shows that the  $R$ -C bond length or the lattice parameter  $a$  is the key distance which modifies  $J_{sf}$ . In a simple model we assume that  $J_{sf}$  increases linearly as the  $a$  lattice parameter shrinks with respect to that of unalloyed  $R\text{Ni}_2\text{B}_2\text{C}$  [33]. Therefore we incorporate by analogy with the hydrostatic pressure effect a linear dependence of the exchange interaction  $J_{sf}(a) = J_{sf0} + (dJ_{sf}/da)\Delta a(1-x)$  as a function of the lattice constant  $a$  into the pair-breaking relation, where  $\Delta a = a_{x=1} - a_{x=0}$  is the lattice parameter difference of the parent compounds. The comparison of the model curves with the experimental data demonstrates that the two parameter account for the chemical pressure describes reasonably well the initial suppression rates of  $T_C$  in the magnetically dilute limit. Even the pronounced curvature in  $T_C(x)$  in  $\text{Lu}_{1-x}\text{Ho}_x\text{Ni}_2\text{B}_2\text{C}$  can be traced back to the release of chemical pressure within this series. This approach explains a number of features of the phase diagrams in Fig. (6) showing that  $N(E_f) \cong 0.34$  states/(eV atom spin) and  $J_{sf0} = 31$  meV ( $340 \text{ meV}\text{\AA}^3$ ) is indeed constant and that the CEF influence as well as the effect of disorder upon the depression of  $T_C(x)$  is small within the *heavy* rare earth series (except Yb).

---

chemical pressure, i.e. when the lattice parameters change due to rare earth substitution in  $\text{R}_{1-x}\text{R}_x\text{Ni}_2\text{B}_2\text{C}$  with  $R = \text{Y, Lu}$ .

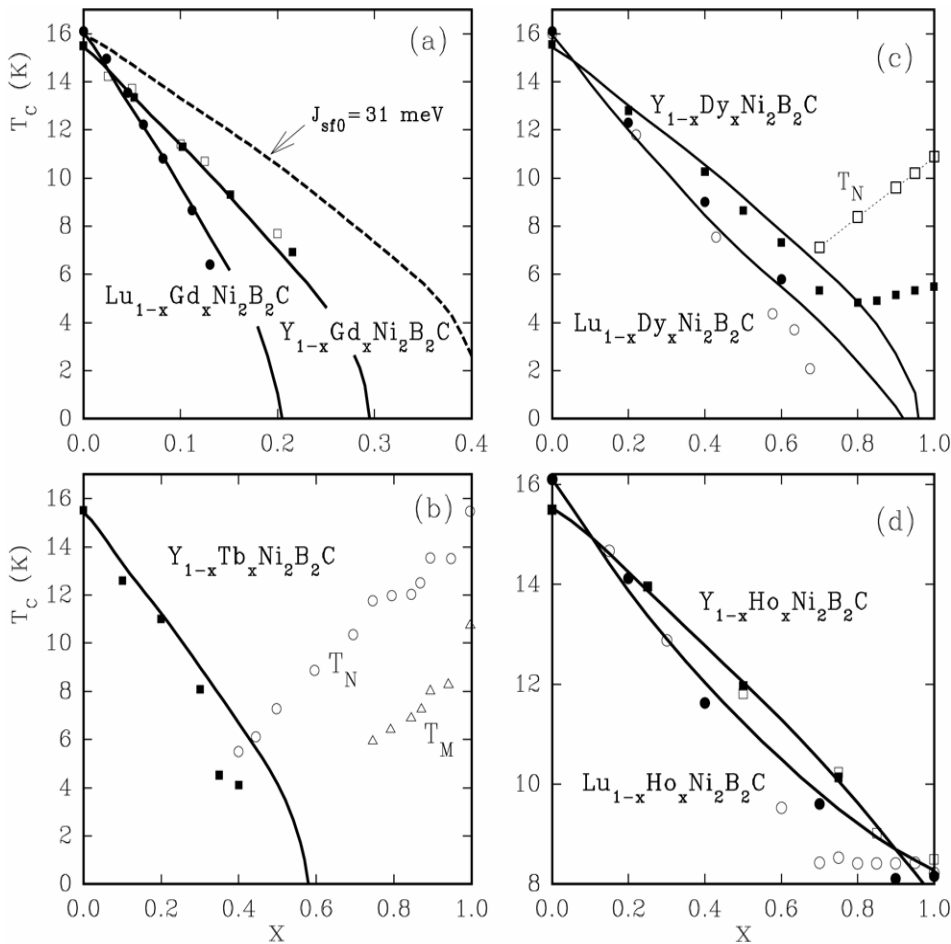


**Fig. (6) :** Comparison of the calculated  $T_c(x)$  (see text) and the experimental data as labeled. The dashed line in (a) corresponds to the AG calculation with  $J_{st0} = 31$  meV for  $\text{Lu}_{1-x}\text{Gd}_x\text{Ni}_2\text{B}_2\text{C}$  without taking into account the chemical pressure.

**Conclusions:**

The thermodynamic properties such as the specific heat jump and thermodynamic critical field as well as the upper critical fields were analyzed within the Eliashberg theory including anisotropy effects, yielding electron phonon coupling anisotropy parameters  $\langle a_k^2 \rangle$  ranging between 0.02 and 0.03 for the whole series, and Fermi velocity anisotropy parameters of  $\langle b_k^2 \rangle \cong 0.25$  in both systems, the borocarbides and boronitride. However, a significantly larger anisotropy of electron-phonon interaction  $\langle a_k^2 \rangle \cong 0.08$  for  $\text{La}_3\text{Ni}_2\text{B}_2\text{N}_{3.5}$  compared to  $\langle a_k^2 \rangle \cong 0.03$  in the single layer borocarbides is observed. The

larger  $\langle a_k^2 \rangle$  explains the weak-coupling signatures of the boronitride, though its coupling strength is of similar magnitude as that of the borocarbides, namely, moderately strong.

The band structure calculations show that a reduction on the density of states on the light rare earth side (in particular for  $R = \text{La}$ ,  $\text{Pr}$ , and  $\text{Nd}$ ) is large enough to explain the suppression of superconductivity to below 3 K for  $\text{Nd}$ ,  $\text{Pr}$ , and  $\text{La}$  while magnetic pair is responsible for the depression of  $T_C$  in the heavy rare earth compounds and their solid solutions with  $\text{Y}$  and  $\text{Lu}$ . This is in line with the analysis of the specific heat anomalies associated with the superconducting transition which show a common correlation between the specific heat jump and superconducting transition temperature with an almost quadratic relation. A simple description which combines the weak coupling results of magnetic pair breaking theory with strong coupling corrections explains reasonably well the quadratic relation between  $\Delta C$  and  $T_C$ . The overall agreement of this simple approach with our experimental data indicates that the  $\gamma$  value and hence the electronic density of states are almost constant in the heavy rare earth borocarbides and their pseudoquaternary solid solutions with  $\text{Y}$ .

The investigation of pair-breaking effects in magnetic rare-earth nickel borocarbide superconductors reveals a considerable increase of the magnetic exchange integral  $J_{sf}$  by hydrostatic as well as chemical pressure. In both,  $J_{sf}$  is governed by the R-C distance (or lattice constant  $a$ ) and is described quantitatively by a simple phenomenological model. Thereby, just two parameters  $J_{sf0} = 31 \text{ meV}$  and  $\Delta J_{sf}/\Delta a = 165 \text{ meV \AA}$  explain well the influence of chemical pressure upon the initial depression rates of  $T_C$  in solid solutions with  $\text{Y}$  and  $\text{Lu}$ .

## Acknowledgements

This work is supported by the Austrian Science Foundation FWF under project P-16250-N02. One of the Authors "M. El-Hagary" would like to thank the OEAD for the support during his stay in Vienna.

**References:**

1. R. Nagarajan, C. Mazumdar, Z. Hossain, S. K. Dhar, K. V. Gopalakrishnan, L. C. Gupta, C. Godart, B. D. Padalia, and R. Vijayaraghavan, *Phys. Rev. Lett.* **72**, 274 (1994).
2. R. J. Cava, H. Takagi, H. W. Zandbergen, J. J. Krajewski, W. F. Peck Jr., T. Siegrist, B. Batlogg, R. B. van Dover, R. J. Felder, K. Mizuhashi, J. O. Lee, H. Eisaki, and S. Uchida, *Nature* **367**, 254 (1994).
3. T. Siegrist, H. W. Zandbergen, R. J. Cava, J. J. Krajewski, and W. F. Peck Jr., *Nature* **367**, 146 (1994); T. Siegrist, R. J. Cava, J. J. Krajewski, and W. F. Peck Jr., *J. Alloy and Compounds* **216**, 135 (1994).
4. L. F. Mattheiss, *Phys. Rev. B* **49**, (13), 279 (1994).
5. W. E. Pickett and D. J. Singh, *Phys. Rev. Lett.* **72**, 3702 (1994).
6. L. Gao, X. D. Qiu, Y. Cao, R. L. Meng, Y. Y. Sun, Y. Y. Xue, and C. W. Chu, *Phys. Rev. B* **50**, 9445 (1994).
7. Li Rukang, X. Chaoshui, Z. Hong, Lu Bin, and Yang Li, *Journal of Alloys and Compounds* **223**, 53 (1995).
8. R. J. Cava, H. W. Zandbergen, B. Batlogg, H. Eisaki, H. Takagi, J. J. Krajewski, W. F. Peck Jr., E. M. Gyorgy, and S. Uchida, *Nature (London)* **372**, 245 (1994).
9. H. W. Zandbergen, J. Jansen, R. J. Cava, J. J. Krajewski, and W. F. Peck Jr., *Nature (London)* **372**, 759 (1994).
10. L. F. Mattheiss, *Solid State Comm.* **94**, 741 (1995).
11. D. J. Singh and W. E. Pickett, *Phys. Rev. B* **51**, 8668 (1995), **51** R 8668-R 8671 (1995).
12. Michor H., Krendelsberger R., Hilscher G., Bauer E., Dusek C., Hauser R., Naber L., Werner D., Rogl P., and Zandbergen H.W., *Phys. Rev. B* **54**, 9408 (1996).
13. Hoellwarth C.C., Kalvins P., and Shelton R.N., *Phys. Rev. B* **53**, 2579 (1996).
14. Michor H., Hilscher G., Krendelsberger R., Rogl, P., and Bouree F., *Phys. Rev. B* **58**, 15 045 (1998)
15. Michor H., Holubar T., Dusek C., and Hilscher G., *Phys. Rev. B* **52**, 16165 (1994).
16. Dugdale S.B., Alam M.A., Wilkinson I., Hughes R.J., Wills H.H., Fisher I.R., Canfield P.C., Jarlborg T., and Santi G., *Phys. Rev. Lett.* **83**, 4824 (1999).
17. Terashima T., Haworth C., Takeya H., Uji S., Aoki H., and Kadowaki K., *Phys. Rev. B* **56**, 5120 (1998).
18. Shulga S.V., Drechsler S. L., Fuchs G., Müller K. H., Winzer K., Heinecke M., and Krug K., *Phys. Rev. Lett.*, **80**, 1730 (1998)
19. Prohammer M. and Schachinger E., *Phys. Rev. B* **36**, 8353 (1987)

20. Manalo S., Michor H., El-Hagary M., Hilscher G., and Schachinger E., Phys. Rev. B **63** 104508-1-12 (2001).
21. Eisaki H., Takagi H., Cava R.J., Batlogg B., Krajewski J.J., Peck F.W., Mizuhashi K., Lee J.O., and Uchida S. Phys. Rev. B **50**, 647 (1994)
22. Lynn J.W., Skanthakumar S., Huang Q., Sinha S.K., Hossain Z., Gupta L.C., Nagarajan R., and Godart C., Phys. Rev. B **55**, 6584 (1997)
23. Hilscher G. and Michor H. Superconductivity and Magnetism in quaternary Borocarbides and Boronitrides, in A.V. Narlikar (ed.), *Studies on High Temperature Superconductors*, Nova Science Publishers, New York, Vol. **28**, 241 (1999).
24. Divis M., Michor H., Khmelevsky S., Blaha P., Hilscher G., and Schwarz K. Phys. Rev. B **62**, 6774 (2000)
25. Fulde P. and Peschl I., Advances in Physics **21**, 1 (1972)
26. Cho B.K., Canfield P.C., and Johnston D.C. Phys. Rev. Lett. **77**, 163 (1996).
27. Freudenberger J., Fuchs G., Nenkov K., Handstein A., Wolf M., Kreyssig A., Müller K.-H., Löwenhaupt M., and Schulz L. Journal of Magn. Magn. Mat. **187**, 309 (1998).
28. El-Hagary M., Michor H., Hilscher G., Phys. Rev. B **61**, 11695 (2000)
29. Skalski S., Betheder-Matibet O., and Weiss P.R., Phys. Rev. A **136**, 1500 (1964).
30. Carbotte J.P., Review of Modern Physics **62**, 1027 (1990)
31. Schmidt H., Braun H.F. Physica C **229**, 315 (1994)
32. Alleno E., Neumeier J.J., Thompson J.D., Canfield P.C., and Cho B. K. Physica C **242**, 169 (1995)
33. Michor H., El-Hagary M., Naber L., Bauer E., Hilscher G. Phys. Rev. B **61**, R, 6487 (2000)